FACULTAD
DE CIENCIAS
DEL MAR

UNIVERSIDAD DE LAS PALMAS
DE GRAN CANARIA

WAVE EVOLUTION IN THE CANARY ISLANDS

Itzíar Rubio Astorga

Curso 2019/2020

Dr. Ignacio Alonso Bilbao
Mariona Casamayor Font

Trabajo Fin de Título para la obtención del título de Máster en Oceanografía.

Wave evolution in the Canary Islands

Trabajo de fin de título presentado por Itzíar Rubio Astorga para la obtención del título de Máster Universitario en Oceanografía por la Universidad de Las Palmas de Gran Canaria, la Universidad de Vigo y la Universidad de Cádiz.

Tutor: Dr. Ignacio Alonso Bilbao, Instituto de Oceanografía y Cambio Global, Universidad de Las Palmas de Gran Canaria.
Cotutora: Mariona Casamayor Font, Instituto de Oceanografía y Cambio Global, Universidad de Las Palmas de Gran Canaria

Itzíar Rubio Astorga | Ignacio Alonso Bilbao | Mariona Casamayor Font

En Las Palmas de Gran Canaria a 15 de junio del 2020

Index

Abstract……………………………………………………………………..Page 4
1 Introduction
1.1 General background……………………………………………………Page 5
1.2 Study area………………………………………………………………Page 6
2 Data and methods………………………………………………...........Page 6
3 Storm definition…………………………………………………..…...Page 8
4 Results
4.1 Buoys vs SIMAR series……………………………………..……Page 9
4.2 Wave evolution……………………………………......……..........Page 14
4.3 Storm Criteria…………………………………………......…..Page 19
4.4 Wave storm evolution……………………………………………...Page 20
5 Discussion…………………………………………………………….Page 21
6 Conclusion……………………………………………………...….Page 24
7 References………………………………………………...……....Page 25
Appendix………………………………….…..………………………......Page 28

Abstract

A large amount of data is currently available to study the waves conditions in a wide part of the world. In Spain, wave data recorded at buoys and SIMAR series can be obtained from Puertos del Estado. The goals of this study are to analyse the differences between both wave data sources, study the evolution of the waves, establish a criterion to define storms and estimate the trend in the Canary Islands. SIMAR series come from the concatenation of SIMAR-44 subset and WANA subset. Results have been calculated in 3 different periods to avoid the effect of the improvements made in the WANA model. The parameters used are Hs and Tp. The criteria followed to define a wave storm was established considering the 99th percentile threshold of Hs at each selected node, a minimum duration of 6 h and an inter-storm period of 48 h. The correlations of Hs are higher with each improvement of the model, contrary to what happens with Tp. Furthermore, the SIMAR data underestimates the Hs values obtained with the buoy. The obtained trends show negative values in Hs and Tp both in the north and south with a decrease of 0.6 and 0.03 cm/year 0.02 and 0.07 s/year, respectively. Regarding storms, the duration presents a positive trend of 0.40 min/year while Hs decreases with an average value of 0.78 cm/year.

Keywords: SIMAR, significant weight height trend, peak period trend, wave storm, climate change

Resumen

Actualmente hay disponible una gran cantidad de datos para estudiar el oleaje en cualquier parte del mundo. En España, los datos de olas registrados en las boyas y series SIMAR se pueden obtener de Puertos del Estado. Los objetivos son analizar las diferencias entre ambas fuentes de datos, estudiar la evolución de las olas, establecer un criterio para definir las tormentas y estimar su tendencia en las Islas Canarias. La serie SIMAR proviene de la concatenación del subconjunto SIMAR-44 y el subconjunto WANA. Los resultados se han calculado en 3 periodos distintos para evitar el efecto de las mejoras realizadas en el modelo WANA. Los parámetros utilizados son Hs y Tp. El criterio usado para definir una tormenta se estableció considerando el umbral del percentil 99 de cada nodo seleccionado, una duración mínima de 6 h y un período entre tormentas de 48 h. Las correlaciones de Hs son más altas con cada mejora del modelo, al contrario de lo que sucede con el Tp. Además, los datos SIMAR subestiman los valores de Hs respecto a la boya. Las tendencias obtenidas muestran valores negativos en Hs y Tp tanto al norte como al sur de las islas con una disminución de 0.6 y 0.03 cm/año y 0.02 y 0.07 s/año respectivamente. En cuanto a las tormentas, la duración presenta una tendencia positiva de 0.40 min/año, mientras que Hs disminuye 0.78 cm/año.

Palabras clave: SIMAR, tendencia altura de ola significativa, tendencia periodo de pico, oleaje de tormenta, cambio climático

1 Introduction.

1.1 General background.

Climate change has become one of the greatest concerns of human beings in recent years. Due to this, during the last decades there has been an increase in the number of investigations on the possible effects of climate change both, in the open ocean and on the coast. In terms of environmental and economic impacts, coastal wave storms are among the most significant on earth because coastal regions represent the most populated areas and, therefore, they represent a great strategic value for the economy and development of a country (Di Paola *et al*., 2020). One immediate consequence of climate change in coastal zones is the modification of the intensity, frequency and location of storms worldwide (Kossin *et al*., 2014).

In the North Atlantic Ocean, there has been a lot of trend analysis of wave storms (Allan and Komar, 2000; Wang and Swail, 2002; Keim *et al*., 2004; Pilar *et al*., 2008) using different hindcast models and having different results depending of the study area. For example, Keim *et al.* (2004) studied the spatial and temporal variability of coastal storms in the North Atlantic Basin where their record shows decadal scale variability, but neither demonstrates highly significant trends that can be linked conclusively to natural or anthropogenic factors.

Numerical models of hindcasting and prediction of oceanographic variables are shown today as an essential tool to analyse the effects of climate change, also, satellite remote sensing and buoys provide an efficient way for monitoring oceanographic parameters. Oceanographic data has been available today since 1958 thanks to the project "Hindcast of Dynamic Processes of the Ocean and Coastal Areas of Europe (HIPOCAST)". The HIPOCAST project database is the most appropriate to study the changes in the Spanish coastal dynamics in the second half of the 20th century (Tomás *et al*., 2004).

Statistical characterization of the sea states in a certain study area is usually carried out with the significant wave height, average peak period and direction of the waves. (Tomás *et al*., 2004). If the hindcast and remote sensed data are available, they must be compared in order to assess the level of uncertainty involved in using the different type of data (Carretero *et al*., 2002).

Taking all this into account, it should be noted that there are very few studies on the trend of wave climate and storms using the oceanographic data obtained by the HIPOCAST project in the Canary Islands. For this reason, the objectives of the current study are:

1. Analyse the differences between both available wave data sources in the study area, SIMAR series data and buoys data, in order to compare the reliability of both data sources.

2. Study the evolution of the waves in the Canary Islands using the data obtained by the SIMAR model and make estimates of future scenarios with the results obtained.
3. Establish a criterion to define storms and study the trend in the Canary Islands.

1.2 Study area.

The present study was carried out in the Canary Islands (Spain), an archipelago formed by eight major volcanic islands. It is located in the Atlantic Ocean about 100 km off African continent between latitude 27º4'-29º6'N and longitude 18º16'-13º23'W (Figure 1). The largest islands are Tenerife and Fuerteventura with a surface area of 2 034 km^2 and 1 660 km^2, respectively. Tenerife and Gran Canaria are the most inhabited.

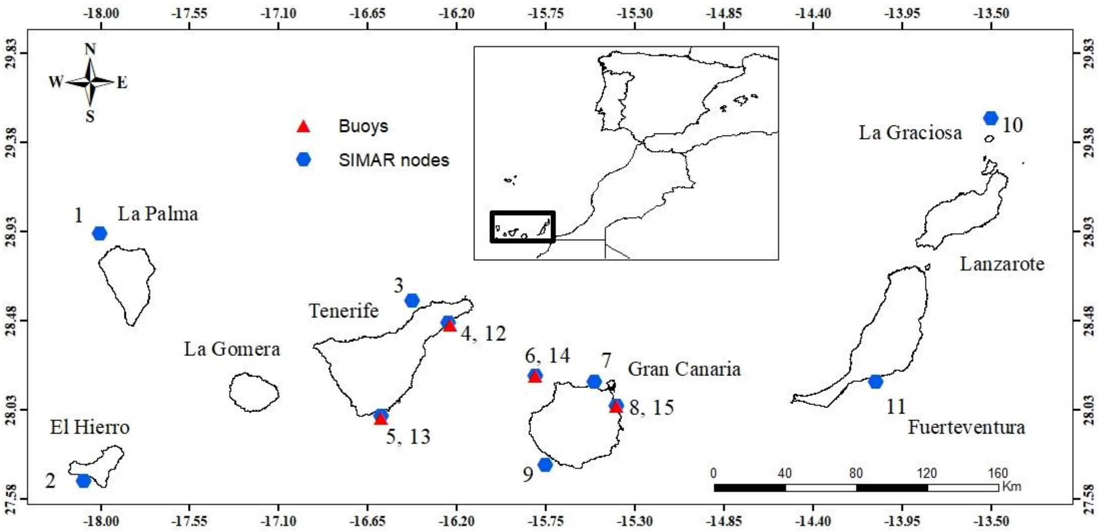

Figure 1. Map of Canary Islands showing the location of the different SIMAR nodes and wave buoys used in this study (Reference system: GCS_WGS_1984).

Regarding wave climate, a cyclical behaviour can be observed on annual time scales, mainly produced by the solar cycle that is known as seasonal variation (Rodríguez *et al.*, 2015). Higher wave heights and periods are more frequent from late fall to early spring. In fact, the presence of the swell is more frequent between October and March. (Yanes *et al.*, 2006). The mean wave direction approaches the islands from WNW to ENE.

2 Data and methods.

To characterize the wave climate, SIMAR data were obtained from the oceanographic database of the Spanish holding of harbours "Puertos del Estado". SIMAR series come from the concatenation of the SIMAR-44 subset, using the numeric model WaveWatch III that provides data from 1958 to 2005 with a resolution of 5'latitude x 5' longitude in the study area, and the WANA subset, based on the use of both, WAM and WaveWatch spectral models of 3rd generation, that provides data from 2006 to actuality. The WANA subset has been improving the spatial and time resolutions of the model over the years as it can be seen in Table 1. More than 60 years of data have been used to characterise the wave climate in the current study which are enough to analyse wave height trend according to Komar and Allan (2008).

Table 1. Evolution in the spatial and time resolution of the wave model that generates the WANA subset.

2006-2011		**2012-2017**		**2018-Present**	
time	spatial	time	spatial	time	spatial
3h	8.3 km	1h	5 km	1h	2.1 km

Having into account our objectives, 7 SIMAR nodes were selected both at the northern and the southern coast of the islands to characterise the whole archipelago (Figure 1). Furthermore, 4 additional SIMAR nodes located as close as possible to the 4 active wave buoys corresponding to REDEXT and REDCOST network were also chosen to make the correlations between SIMAR and buoys data (Table 2).

Table 2. Locations, codes, and names of the SIMAR nodes and buoys selected.

Id	Source	Code	Lat (Nº)	Long (Wº)	Name
1	SIMAR	4006026	29'42º	18'00º	La Palma N
2	SIMAR	4005005	27'67º	18'08º	El Hierro SW
3	SIMAR	4025016	28'58º	16'42º	Tenerife N
4	SIMAR	415033026	28'47º	16'24º	Santa Cruz de Tenerife
12	BUOY	1421	28'46º	16'23º	Santa Cruz de Tenerife
5	SIMAR	4023009	28'00º	16'58º	Tenerife S
13	BUOY	2446	27'99º	16'58º	Tenerife S
6	SIMAR	1017013	28'20º	15'80º	Gran Canaria NW
14	BUOY	2442	28'20º	15'80º	Gran Canaria NW
7	SIMAR	4036011	28'17º	15'50º	Gran Canaria N
8	SIMAR	421038045	28'05º	15'39º	Las Palmas E
15	BUOY	1414	28'05º	15'39º	Las Palmas E
9	SIMAR	4033006	27'75º	15'75º	Gran Canaria SW
10	SIMAR	1026018	29'50º	13'50º	Lanzarote N
11	SIMAR	4053011	28'17º	14'08º	Fuerteventura S

It must be considered that not all SIMAR nodes or buoys have the same data number. In general, all SIMAR nodes present hourly data from 04/01/1958 to 13/11/2019 (the day the data was requested to Puertos del Estado), except for SIMAR number 4 and 8, whose data runs from 19/09/2012 to 13/11/2019.

In the case of buoys, number 12 has data from 22/05/2009, number 13 began on 01/04/1998 and number 15 presents data from 02/05/1992, these three buoys recorded data until 13/11/2019. Finally, the number 14 buoy, has data from 20/06/1997 to 27/09/2019 because of operational problems. For this reason, the wave climate evolution and storm study are carried out with the data obtained by the SIMAR series because it has a greater number of data compared to the buoy data.

The parameters used are, both for SIMAR nodes and buoys, significant wave height (m), peak period (s) and mean wave direction (º). Data frequency is 1 hour in any case except for buoy data recorded before 1999. In that case the record includes one data every 3 hours.

Several correlations were made between SIMAR series data and buoys data to be able to study which factors/variables are the ones that differ between the two groups of data. To study and characterize the temporal trend, duration, and direction of wave storms in the study area, several time series have been carried out for each of the nodes of both, the heights and the peak periods. In addition to the joint analysis of the data, the trend has been calculated in three different periods of the time series in order to minimize the effect of the model in the trend calculation. As the last spatial resolution improvement was made in 2018, the number of data from that date to the present is very short, so this improvement will not be taken into account as the results could be influenced by the seasonality of the data. Therefore, trends were calculated in the following periods: 1958-2005; 2006-2011 and 2012-2019. Regarding storms, the cumulative time per year was computed by adding up the total number of hours in a certain year in which the defined storm threshold was reached. All figures were made by Excel and Grapher 13 except Figure 1 which was made with ArcGIS 10.4.1.

3 Storm definition

A storm can be defined as a wave event in which the significant wave height (Hs) exceeds a certain threshold during a certain period of time (Mendoza *et al.*, 2011). There is no globally accepted criterion for defining a storm, the selection of the parameters wave height threshold, minimum duration above threshold and minimum inter-storm period depends on local characteristics. A large variability in the criteria used to define a storm wave can be observed in literature (Table 3).

Table 3. Literature review with the criteria used in each case to define a storm wave.

Reference	Significant Wave Height Threshold (m)	Minimum duration (h)	Minimum inter-storm period (h)
Rangel-Buitrago and Anfuso (2013)	2.5	12	24
Anfuso *et al*. (2016)	2.5	12	24
Grottoli *et al*. (2017)	1.5	6	3
Ojeda *et al*. (2017)	$\langle SwH \rangle + 2\sigma$	12	48
Ciavola and Coco (2017)	Hs > Hs,99%	6	24
Godoi *et al*. (2018)			72
Nose *et al*. (2018)	4		
Di Paola *et al*. (2020)	2 (west) / 3 (east)	3	48

In Canary Islands, different wave climate conditions are found in every island, therefore Hs thresholds vary in each selected node. A way to obtain Hs thresholds characteristic of the study area is to select them based on percentiles (Godoi *et al*., 2018). Peaks-over-threshold were used to identify storm wave events considering the 99^{th} percentile threshold of each selected node. In addition, a threshold height per period was defined to minimize the effect of improvements when studying storms. The total length of the data set was used in each node.

4 Results

4.1 Comparison between buoy data and SIMAR data.

To compare the data measured in the buoy with the data obtained in SIMAR visually, time series were performed for each study area where the buoy and SIMAR node coincided. They were performed with the one-month running average for each data set (i.e. 720 data).

It can be seen in Figure 2 that in any location both time series follow a similar pattern, with high and low values taking place simultaneously. Nevertheless, a closer view shows that in Santa Cruz de Tenerife, SIMAR wave height data tends to be underestimated relative to buoy data. In Tenerife S three periods can be identified: from 1998 to 2005 SIMAR significant wave height data are clearly underestimated compared to the buoy data; from 2006 to 2011 wave heights of SIMAR model increase to be almost on a par with those recorded by the buoy, and finally, from 2012 onwards, both data series show practically equal values. At last, in Gran Canaria NW and Las Palmas E, both data series obtain similar values of wave height.

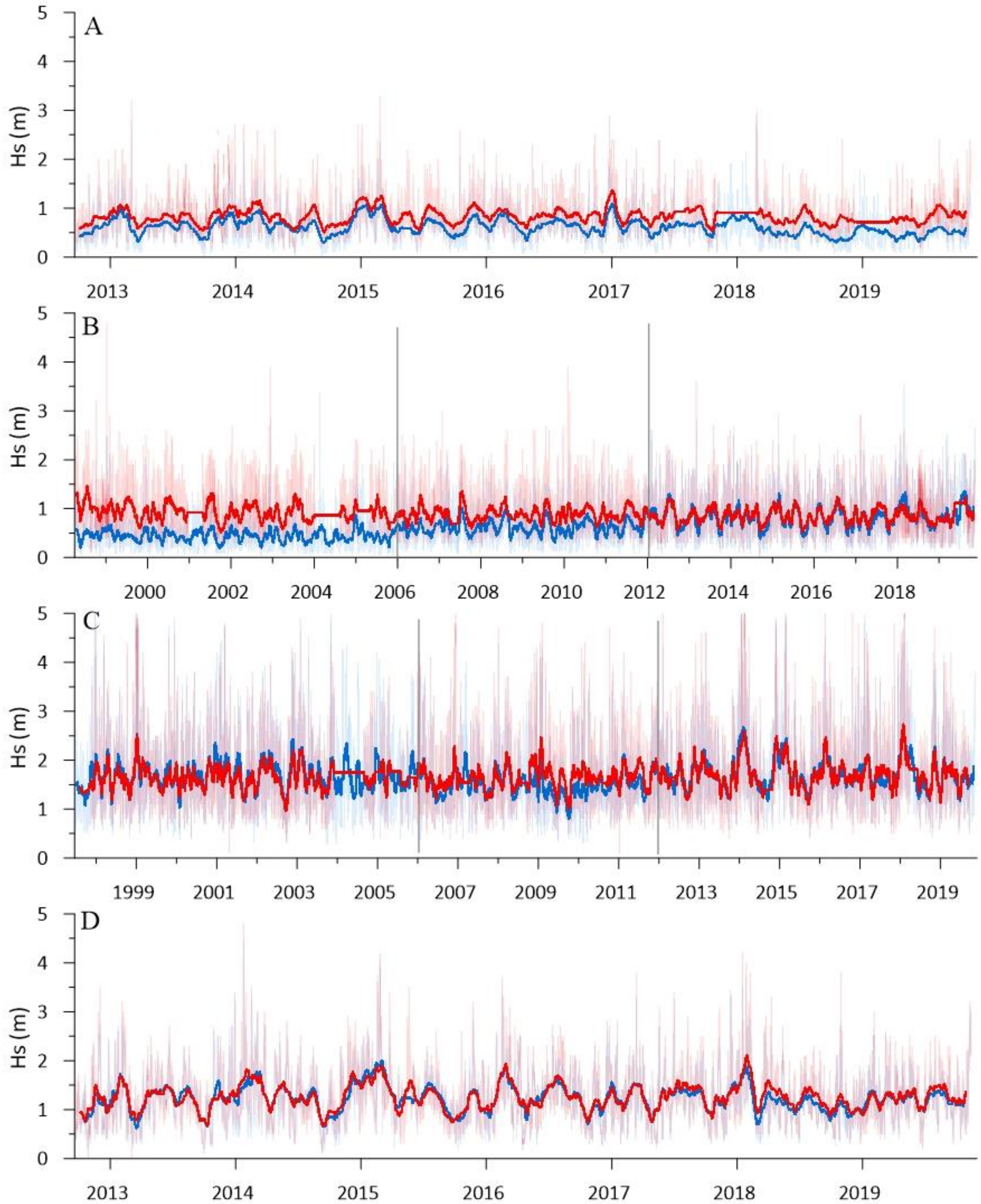

Figure 2. Time series with running average of SIMAR series in blue colour and running average of buoys data in red colour, in (A) Santa Cruz de Tenerife, (B) Tenerife S, (C) Gran Canaria NW and (D) Las Palmas E. Vertical lines separate the different periods considered based on modifications to the WANA model.

To make the correlations, buoys data have been represented on the X axis and SIMAR series data on the Y axis, because the data obtained *in situ* by the buoy are considered the most reliable one. Four correlations of the wave height data were performed (Figure 3) and the results obtained statistically can be observed in Table 4.

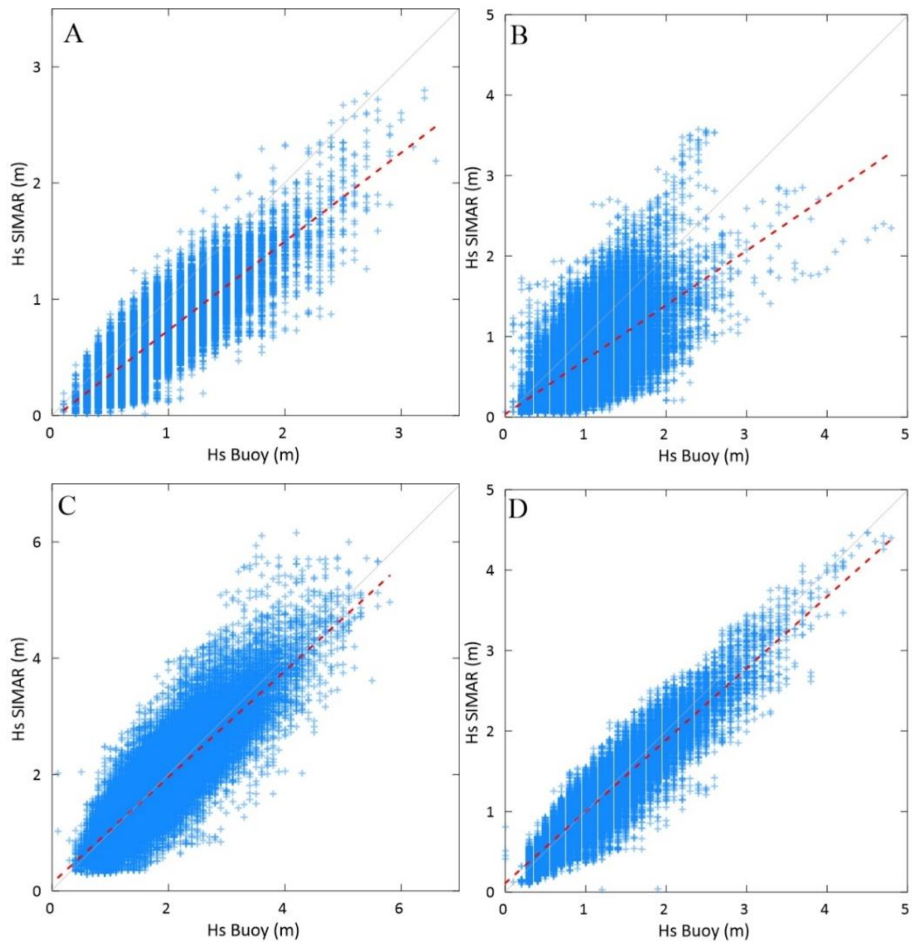

Figure 3. Correlations between significant wave heights obtained from SIMAR series data and buoys data in (A) Santa Cruz de Tenerife, (B) Tenerife S, (C) Gran Canaria NW and (D) Las Palmas E.

Figure 3 shows the correlations that were obtained between the buoys and the SIMAR nodes. In Table 4, it can be seen that the best correlation is found in Las Palmas E followed by Gran Canaria NW, Santa Cruz de Tenerife and finally, Tenerife S.

The three best correlations are exposed to northern and eastern waves, unlike the worst (Tenerife S) that is found at the south. This coincides with the time series observed in Figure 2 where Tenerife S has visually the greatest differences in significant wave height with SIMAR series.

Correlations have also been made by periods in both Tenerife S and Gran Canaria and as it can be seen in Table 4, the correlations are better by period than in general. In turn, it can be noticed how the correlation increases as the model improves in the case of Tenerife S and the average differences between the buoy and the SIMAR values are reduced. In both Tenerife S and Gran Canaria NW, the best correlation coefficient is obtained in the last period (2012-2019), which coincides with the last two improvements of the model.

Table 4. Results of the significant wave height correlation between the buoys and the SIMAR nodes.(N= nº of data; Δ= average differences between the buoy and SIMAR values).

		R	Δ	N			R	Δ	N
SC Tenerife		0.857	0.226±0.185	54 359	**GC NW**	**Total**	0.872	0.010±0.313	168 912
Tfe S	**Total**	0.663	0.252±0.308	168 409	**GC NW**	**1997-2005**	0.890	-0.068±0.311	59 719
Tfe S	**1998-2005**	0.752	0.498±0.259	54 751	**GC NW**	**2006-2011**	0.839	0.148±0.672	46 712
Tfe S	**2006-2011**	0.782	0.273±0.227	47 288	**GC NW**	**2012-2019**	0.905	-0.018±0.595	62 481
Tfe S	**2012-2019**	0.839	0.035±0.226	66 370	**Las Palmas E**		0.921	0.027±0.208	59 980

Another possible factor that affects the correlation could be that SIMAR series do not estimate high significant wave heights well. For this reason, correlations were made in different significant wave height intervals. Furthermore, correlations by period were also obtained and the results (Table 5) were quite ambiguous.

Table 5. Results of the correlation between the buoys and SIMAR data in every significant wave height. Subscripts 1, 2 and 3 corresponds to the three periods considered: 1958-2005, 2006-2011, and 2012-2019. No subscript corresponds to the whole data set.

	R_1	N_1	R_2	N_2	R_3	N_3	R	N
SC de Tenerife								
0 > Hs >=1					0.733	65 010	0.733	65 010
1 > Hs >=2					0.613	18 811	0.613	18 811
2 > Hs >= 3.4					0.584	586	0.584	586
Tenerife S								
0 > Hs >=1	0.837	35 707	0.971	34 380	0.728	46 494	0.545	118 141
1 > Hs >=2	0.689	19 128	0.916	14 397	0.739	17 391	0.299	51 687
2 > Hs >= 3	0.337	399	0.886	244	0.712	235	0.253	897
3 > Hs >= 4.8	0.444	20	0.005	12	0.013	5	0.120	36
GC NW								
0 > Hs >=1	0.087	8 527	0.133	6 354	0.218	6 934	0.461	22 177
1 > Hs >=2	0.323	39 373	0.216	31 720	0.225	38 384	0.654	110 835
2 > Hs >= 3	0.256	10 943	0.077	9 238	0.180	12 860	0.524	33 469
3 > Hs >= 4	0.164	1 226	0.082	995	0.153	1 860	0.445	4 159
4 > Hs >= 5.8	0.090	148	0.217	99	0.123	252	0.455	560
Las Palmas E								
0 > Hs >=1					0.747	99 616	0.747	99 616
1 > Hs >=2					0.744	109 127	0.744	109 127
2 > Hs >= 3					0.660	11 479	0.660	11 479
3 > Hs >= 4.9					0.743	676	0.743	676

In general, it can be observed that the quality of the correlation follows the same pattern as that obtained in the previous case, with Las Palmas E being the best correlated, followed by Santa Cruz de Tenerife, Tenerife S and Gran Canaria NW. In the case of Santa Cruz de Tenerife and Tenerife S, both follow the same pattern, decreasing the correlation coefficient as the significant wave height increases even in the three different periods, where the correlation of Tenerife S is higher in the three periods than in general. However, in the case of Gran Canaria NW and Las Palmas E, the correlation coefficients remain practically the same at the different significant wave heights in general. But, in the first and third period a decrease in the correlation coefficient can be seen in Gran Canaria NW unlike the second period that does not follow a pattern.

Peak period data were also correlated between buoys and SIMAR series (Figure 4). In this case, as it can be noticed in Table 6, there is a large difference between the correlation coefficient of Gran Canaria NW and Las Palmas E with Santa Cruz de Tenerife and Tenerife S. Gran Canaria NW is the best correlated followed by Las Palmas E, Santa Cruz de Tenerife, and Tenerife S. Furthermore, in Tenerife S the correlation coefficient and average differences decreases in each period, the opposite of what happened with significant wave height. In Gran Canaria NW, the correlation gets worse in the second period but improves in the third one.

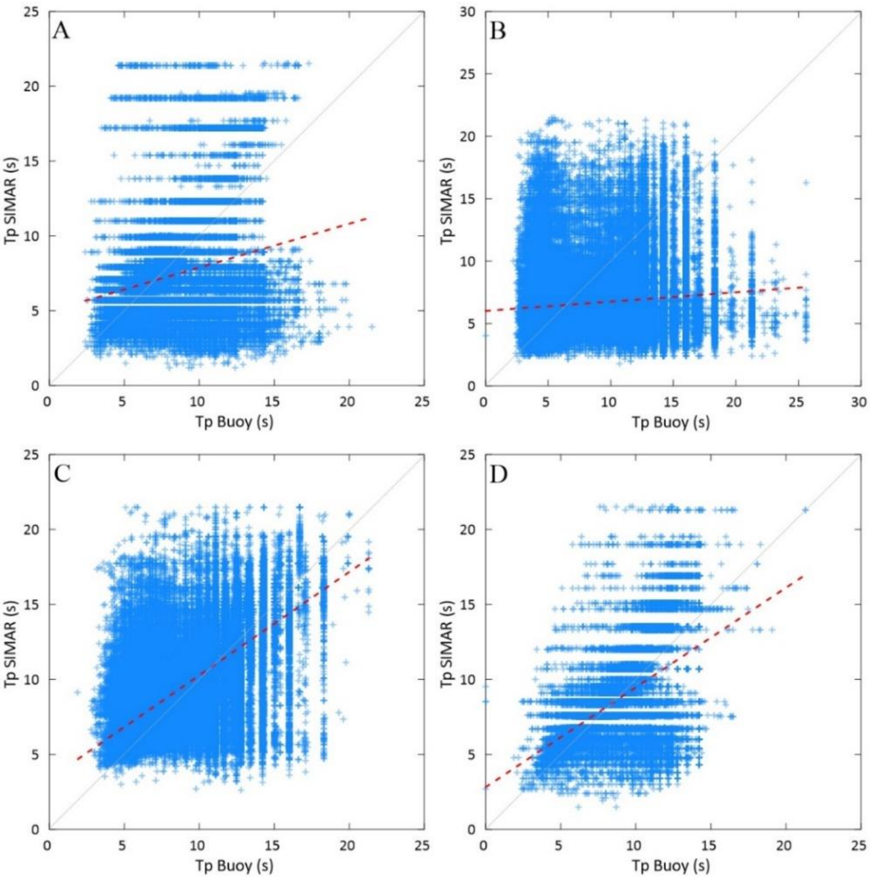

Figure 4. Correlations between peak periods obtained from SIMAR series data and buoys data in (A) Santa Cruz de Tenerife, (B) Tenerife S, (C) Gran Canaria NW and (D) Las Palmas E.

Table 6. Results of the correlation between the obtained Tp (peak period) from buoys and SIMAR nodes (N= nº of data; Δ= average differences between the buoy and SIMAR values).

<table>
<tr><th></th><th></th><th>R</th><th>Δ</th><th>N</th><th></th><th></th><th>R</th><th>Δ</th><th>N</th></tr>
<tr><td colspan="2">SC Tenerife</td><td>0.268</td><td>0.592±3.515</td><td>54 359</td><td rowspan="4">GC NW</td><td>Total</td><td>0.620</td><td>-0.482±2.369</td><td>168 912</td></tr>
<tr><td rowspan="4">Tfe S</td><td>Total</td><td>0.119</td><td>1.383±4.304</td><td>168 409</td><td>1997-2005</td><td>0.693</td><td>-0.383±1.964</td><td>59 719</td></tr>
<tr><td>1998-2005</td><td>0.188</td><td>0.276±3.764</td><td>54 751</td><td>2006-2011</td><td>0.462</td><td>0.182±2.909</td><td>46 712</td></tr>
<tr><td>2006-2011</td><td>0.140</td><td>1.918±4.290</td><td>47 288</td><td>2012-2019</td><td>0.715</td><td>-1.075±2.115</td><td>62 481</td></tr>
<tr><td>2012-2019</td><td>0.095</td><td>1.914±4.548</td><td>66 370</td><td colspan="2">Las Palmas E</td><td>0.588</td><td>-0.148±2.172</td><td>59 980</td></tr>
</table>

In all the correlations made (significant wave height, significant wave height intervals and peak period) the area that obtained the worst results was Tenerife S. In addition, it has been possible to verify with the correlations by significant wave height interval, that the correlation between the two data series does not get worse with a higher wave height at the two study nodes found on the island of Gran Canaria. However, it has been possible to observe how the correlation of significant wave heights in the case of Tenerife S has improved with each period studied, which coincides with what has been observed in the time series in Figure 2. But, in the correlation in peak periods, Tenerife S gets worse with the improvements made.

4.2 Wave Evolution

Wave roses have been represented in each of the SIMAR nodes in order to study the direction of the waves. These roses have been divided into three main groups that follow similar patterns, the most representative roses of each group are in Figure 5. First, there are the SIMAR nodes located to the north and that they have a northern wave origin, ranging from NW to NE (La Palma N, Tenerife N, Gran Canaria NW, Gran Canaria N and Lanzarote N). Secondly, there are the SIMAR nodes located to the southwest protected from the northeast winds by the islands and with northwest direction of origin of the waves (El Hierro SW and Gran Canaria SW). Finally, the SIMAR nodes located to the east of the islands and exposed to eastern waves (Santa Cruz de Tenerife, Tenerife S, Las Palmas E and Fuerteventura S).

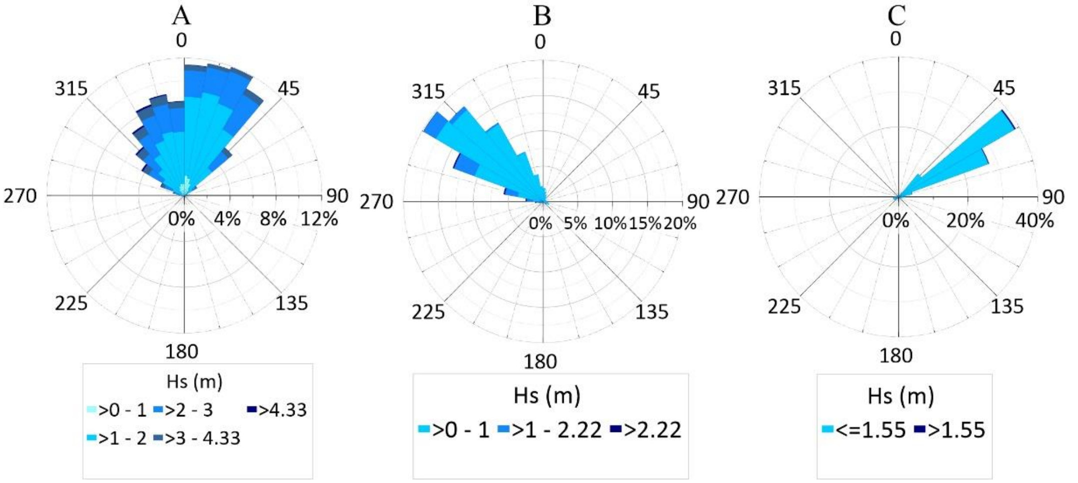

Figure 5. Wave roses in (A) La Palma N, (B) El Hierro SW and (C) Tenerife S. The last wave height interval corresponds to the storm wave height threshold calculated for each of the nodes.

Several time series have been carried out at each selected SIMAR node. They were performed with the one-month running average for each data set (i.e. 720 data). These time series have been divided between those exposed to northern waves (Figure 6) and those protected from northern waves and therefore mostly exposed to southern and eastern waves (Figure 7).

As previously mentioned, all SIMAR nodes have the same data number except for Santa Cruz de Tenerife (Figure 6C) and Las Palmas E (Figure 7B). These two SIMAR nodes are only affected by the latest improvements made to the model since they began operating in 2012. It is possible to see very clearly the seasonal changes where the highest significant wave heights occur during the winter season.

In the rest of the cases, the trends have been calculated considering the different periods described above. Table 7 shows the results of the trends of the SIMAR nodes exposed to northern waves.

On the one hand, in La Palma N (Figure 6A), Tenerife N (Figure 6B) and Gran Canaria N (Figure 6D), a positive trend is observed in the first period, in the second period a negative trend and finally in the third period again, a positive trend in significant wave height. On the other hand, Gran Canaria NW (Figure 6C) shows a positive trend from 1958 to 2005 and a negative trend in the last two periods, from 2006 to the present. Finally, in Lanzarote N (Figure 6F) a negative trend is observed throughout the entire time series. It is worth noting the fact that during the second period all trends are negative.

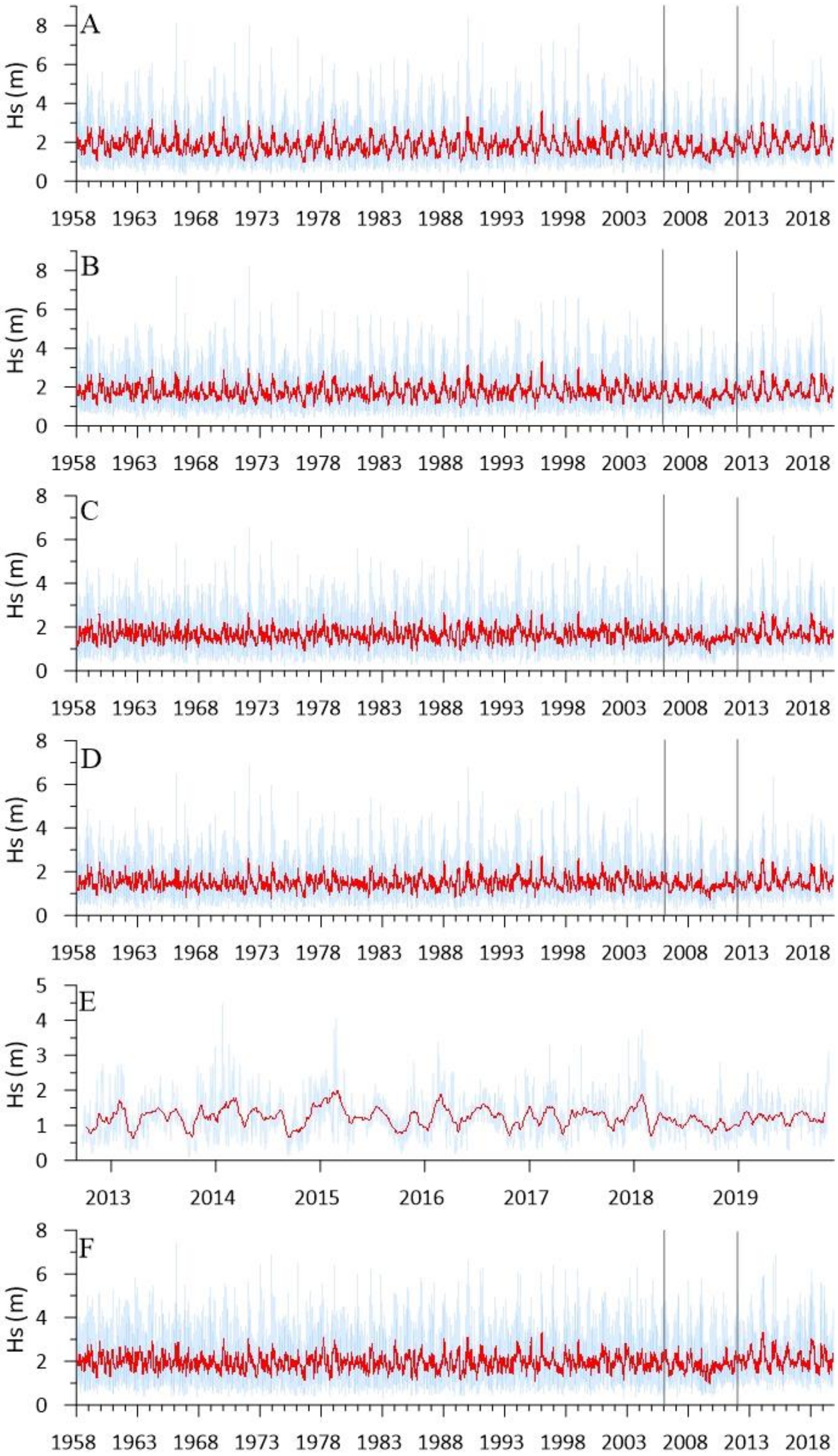

Figure 6. Time series of SIMAR series data in (A) La Palma N, (B) Tenerife N, (C) Gran Canaria NW, (D) Gran Canaria N, (E) Las Palmas E and (F) Lanzarote N. In red colour the running average and in blue colour the data. Vertical lines separate the different periods considered based on modifications to the WANA model.

Table 7. Results of significant wave height trends in SIMAR nodes exposed to northern waves (cm/year).

Id	Name	(1958-2005)	(2006-2011)	(2012-2019)
1	La Palma N	0.060	-1.385	0.467
3	Tenerife N	0.033	-1.777	0.249
6	Gran Canaria NW	0.049	-1.113	-0.986
7	Gran Canaria N	0.047	-1.640	0.577
8	Las Palmas E			-0.718
10	Lanzarote N	-0.045	-2.334	-0.726

As in Figure 6, a clear seasonality can be observed in Figure 7. This seasonality is very marked in El Hierro SW (Figure 7A) where there is a great difference between high and low values. In the case of the SIMAR nodes located to the south, the effect of the model improvements can be visually observed. As in the previous figure, the trends have been calculated in three different periods and the results are shown in the Table 8.

Table 8. Results of significant wave height trends in SIMAR nodes located to the south in cm/year.

Id	Name	(1958-2005)	(2006-2011)	(2012-2019)
2	El Hierro SW	-0.019	-0.734	0.449
4	Santa Cruz de Tenerife			-2.091
5	Tenerife S	0.013	0.456	0.996
9	Gran Canaria SW	-0.018	0.843	-1.102
11	Fuerteventura S	0.026	0.646	-0.334

A negative trend can be observed in the first two periods of El Hierro from 1958 to 2011, and in the last period a negative trend is observed. In the case of Tenerife S, the trend is positive throughout the entire time series. In Gran Canaria SW, negative trends are observed in the first and third periods and positive trend from 2006 to 2011. Santa Cruz of Tenerife has a huge negative trend of more than 2 cm per year. Finally, the significant wave height trend in Fuerteventura S is positive from 1958 to 2011, that is, in the first two periods, but, since 2012 this trend is negative.
It should be noted that the SIMAR nodes located to the south present greater visual differences between the different periods, this could be because they have been more affected by the improvements.

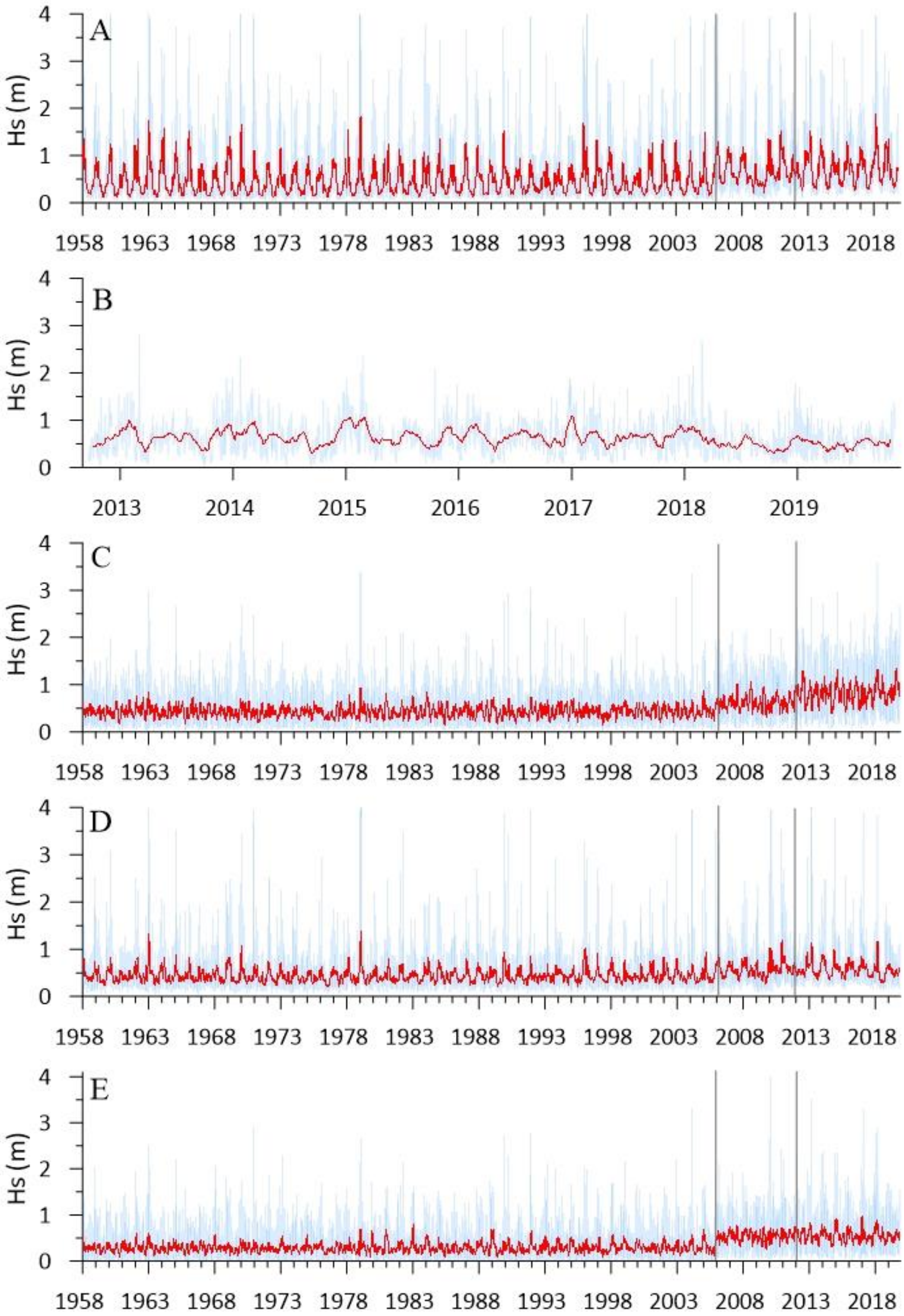

Figure 7. Time series of SIMAR series data in (A) El Hierro SW, (B) Santa Cruz de Tenerife, (C) Tenerife S, (D) Gran Canaria SW, and (E) Fuerteventura S. In red colour the running average and in blue colour de data. Vertical lines separate the different periods considered based on modifications to the WANA model.

Time series were also carried out with the variable peak period (Annex I) and the results of the trends in every period are in Table 9. In general, the trends are positive in the majority except in the second period that presents the greatest number of negative trends, with the exception of Tenerife S and Fuerteventura S, they present a negative trend from 1958 to 2005 and a positive trend in the last two periods, that is, from 2006 to 2019. These two SIMAR nodes are the ones that presented the greatest differences in significant wave height in Figure 6. Santa Cruz de Tenerife and Las Palmas E only have data from 2012 to 2019 and a negative trend is observed in the third period in both cases.

Table 9. Results of peak period trends in SIMAR nodes in s/year.

Id	Name	(1958-2005)	(2006-2011)	(2012-2019)
1	La Palma N	0.003	-0.116	0.033
2	El Hierro SW	0.004	-0.237	0.070
3	Tenerife N	0.003	-0.098	0.066
4	Santa Cruz de Tenerife			-0.255
5	Tenerife S	-0.007	0.024	0.004
6	Gran Canaria NW	0.003	-0.110	0.027
7	Gran Canaria N	0.003	-0.073	0.010
8	Las Palmas E			-0.019
9	Gran Canaria SW	0.005	-0.309	-0.133
10	Lanzarote N	0.003	-0.094	0.037
11	Fuerteventura S	-0.007	0.004	0.011

4.3 Storm Criteria

A minimum duration of a wave storm of 6 h and an inter-storm period of 48 h was established to separate consecutive storm events in order to assure that the events are statistically independent (Dorsch *et al.*, 2008).

Table 10. Values of significant wave height threshold, minimum duration and minimum inter-storm period calculated in each node.

Id	Hs Threshold (m)	Name	Id	Hs Threshold (m)	Name
1	4.33	La Palma N	6	3.69	GC NW
2	2.22	El Hierro SW	14	3.60	GC NW
3	4.02	Tenerife N	7	3.50	GC N
4	1.54	SC Tenerife	8	2.69	Las Palmas E
12	1.90	SC Tenerife	15	2.60	Las Palmas E
5	1.55	Tenerife S	9	1.58	GC SW
13	1.90	Tenerife S	10	4.33	Lanzarote N
			11	1.23	Fuerteventura S

As it can be seen, the highest significant wave height thresholds are generally found in areas exposed to northern waves. Comparing the thresholds obtained in the SIMAR nodes and in the buoys, in the case of the two nodes selected on the island of Gran Canaria, the wave height threshold obtained in the buoys is smaller than the obtained in SIMAR nodes. Nevertheless, in the case of the two nodes selected on the island of Tenerife, the calculated threshold height is higher at the buoys than at the SIMAR nodes and the differences between the calculated threshold of the model and the buoy are considerably greater.

4.4 Wave Storm Evolution

The storm wave evolution in the study area has been carried out taking into account the criteria established to define a storm and the values of the Significant Wave Height Threshold (m), Minimum duration (h) and Minimum inter-storm period (h) parameters in each of the SIMAR nodes (Table 10).

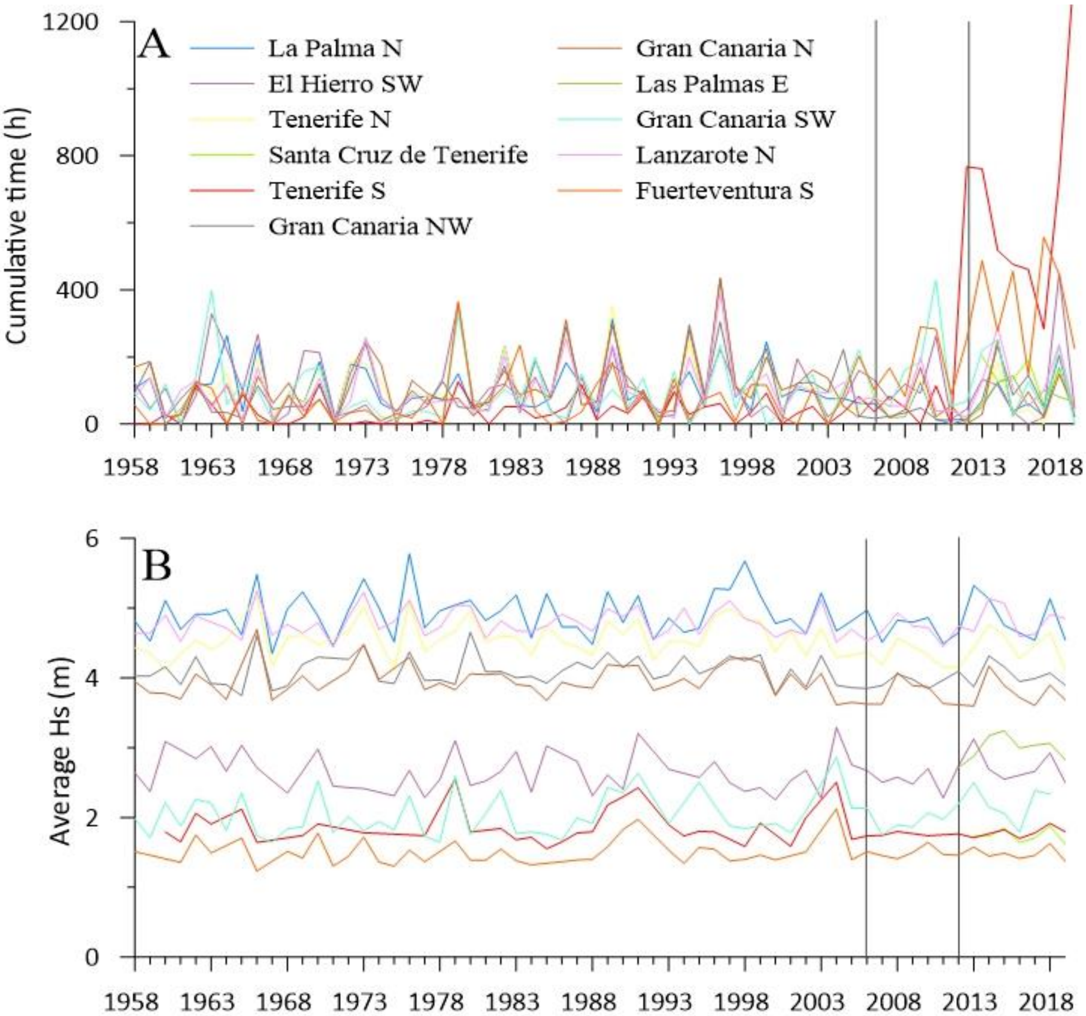

Figure 8. (A) Cumulative time during storm waves per year at each SIMAR node and (B) significant wave height average per year at each SIMAR node. Vertical lines separate the different periods considered based on modifications to the WANA model.

On the one hand, the trend of the cumulative duration of storms per year at each SIMAR node has been studied and can be seen in Figure 8A and, on the other hand, the average significant wave height per year has been represented in Figure 8B. As in the wave climate evolution, the trends have been calculated in three different periods so that the results are not influenced by the improvements in spatial and time resolution of the WANA model.

As it can be seen in Figure 8A, there is a certain cyclicality between years with the highest and lowest cumulative storm time. In addition, Tenerife S and Fuerteventura S stand out in the last section, from 2012 to 2019, since the cumulative storm time increases significantly.

Regarding Figure 8B, on the one hand, there are the SIMAR nodes with the highest significant wave height averages, which are La Palma N, Lanzarote N, Tenerife N, Gran Canaria NW, and Gran Canaria N. These SIMAR nodes coincide with highly exposed areas to northern waves as it is described in section 4.1. On the other hand, the rest of the SIMAR nodes present a significant wave height average lower than the other group. These SIMAR nodes are in areas with less exposure to northern waves and they are Las Palmas E, El Hierro SW, Gran Canaria SW, Tenerife S, Santa Cruz de Tenerife, and Fuerteventura S.

Table 11. Results of cumulative time trends and significant wave height trends in SIMAR nodes during storm waves.

Id	**Cumulative Time (h/year)**			**Hs (cm/year)**		
	(1958-2005)	**(2006-2011)**	**(2012-2019)**	**(1958-2005)**	**(2006-2011)**	**(2012-2019)**
1	0.0011	-0.0128	0.0110	0.037	-6.935	-1.168
2	-0.0020	-0.0024	0.0423	-0.292	-0.365	-1.460
3	0.0020	-0.0143	0.0057	0.183	-2.957	0.037
4			-0.0530			0.402
5	0.0013	-0.0110	0.1113	-0.146	-0.329	-1.132
6	0.0042	-0.0073	0.0081	-0.110	-0.368	-3.322
7	0.0030	0.0025	0.0096	0.073	3.285	-6.607
8			0.0112			-2.555
9	-0.0004	0.0808	-0.0312	0.150	-0.015	-2.227
10	0.0026	-0.0076	0.0014	-0.073	1.095	-1.102
11	0.0025	0.0377	0.0045	-0.084	1.825	-0.219

In general, a positive trend can be observed in most SIMAR nodes with respect to the cumulative time of storms wave per year. However, the significant wave height average during storms waves shows a negative trend in almost all SIMAR nodes in the third period (2012-2019) with the exception of Tenerife N and Las Palmas E.

5 Discussion

Oceanographic data obtained *in situ* by buoys have great scientific value, but the lack of spatial coverage, the short length of the time series, maintenance problems and the consequent loss of data leads to the need to carry out studies with data obtained from models.

Sometimes these models also present problems when measuring as occurs in the model used in this work since, as observed in Figure 2, the data obtained by SIMAR series underestimates the values obtained by the buoys. This also can be seen in Table 4 with the calculated average differences between buoy and SIMAR values, positive values indicate that the buoy generally has higher significant wave height values than SIMAR. In addition, Table 5 shows how the correlations made by height intervals, in the two nodes selected in Tenerife, the coefficient decreases as the significant wave height is higher and, according to Puertos del Estado (2019), data obtained by SIMAR series tend to underestimate wave heights in extreme weather situations. This underestimation has been studied in detail by Bidlot *et al*. (2002) between the data obtained by buoys and the data obtained with different models. These differences between the results of the models and the measurements are due to the limitations inherent in any numerical model (Tomás *et al.*, 2004).

Due to this, the WANA model has undergone improvements over time and these improvements can be clearly seen in Figure 2B, in Tenerife S, where the SIMAR data have been adjusted to what was obtained from the buoy with every improvement. In general, the correlations between buoys and SIMAR data have obtained high values except for Tenerife S, this could be due to the fact that according to Puertos del Estado (2019) at the south of the Canary Archipelago, southwest conditions may not reproduce well due to the proximity of the mesh domain boundary used by the model, and therefore the data obtained by the model in this area correlate worse with the obtained *in situ* by the buoy. Nevertheless, these improvements do not seem to affect the peak period since as it can be seen in Table 6, in the case of Tenerife S, the correlation decreases with each period and the mean difference between the buoy and SIMAR values increases.

Despite the deficiencies mentioned above, the study of trends must be carried out with a long-term database to be able to study with sufficient rigor the effects of climate change (Tomás *et al*., 2004). According to Wang *et al*. (2004) significant wave height in North Atlantic Ocean will tend to increase both the seasonal mean and extreme cases in the 20th century. However, these changes will be accompanied by negative trends in the mid latitudes of the North Atlantic, such as the Canary Islands. This negative trend coincides with the results obtained by Young *et al*. (2011) also in North Atlantic Ocean. In the case of the significant wave height trends obtained in this study, no specific pattern is seen in the behaviour of the trend at the different SIMAR nodes as it can be seen in Tables 7 and 8. On the one hand, the observed long-term trend, which runs from 1958 to 2005, have positive trends in most areas. On the other hand, regarding the short-term trend, which runs from 2006 to 2019 presents a clear negative trend in all nodes except Tenerife S and Lanzarote S, which coincides with the predictions studied for the years 2026- 2045 according to the RCP4.5 scenario where the trend in significant wave height is to decrease or remain except for the southern zone (Ramírez *et al.*, 2019).

Regarding the peak period, the long-term trend is positive in all SIMAR nodes except for Tenerife S and Fuerteventura S where it is slightly negative. However, in the short-term trend (from 2006 to 2019), all SIMAR nodes show negative trends with the exception of Tenerife S and Fuerteventura S, which, in this case, show a slight positive trend. The increase in the period trend means that the swell has increased. In the Canary Islands the swell come from storms located in the low-pressure system of Iceland (Herrera, 2013). According to Ramírez *et al*. (2019), by the year 2100 following the RCP8.5 scenario to study the worst possible future climate impacts, both significant wave height and peak period will tend to decrease (Table 12). Nevertheless, considering the trends obtained in this study, the significant wave height will increase in the north and in the south but, peak period will increase in the north but in the south, it will decrease. These trends present higher values in the north than in the south in both studies.

Table 12. Results obtained for predictions by the year 2100.

	Present study		**Ramírez *et al*. (2019)**	
	Hs (cm)	**Tp (s)**	**Hs (cm)**	**Tp (s)**
North	2.46	0.24	-3.64	-0.21
South	0.03	-0.10	-1.67	-0.03

It can be deduced that the results obtained by Ramírez *et al*. (2019) are more correct to make predictions about climate change since the data used have undergone an adequate calibration, however, the trends used in this study for Table 12 are those corresponding to the first period, which present poor spatial and time resolution.

In the Canary Islands, the duration of wave storms follows a clear positive trend from 1958 to 2005 and from 2012 to 2019, which reach up to almost 7 minutes per year in the case of Tenerife S. Again, negative trends are grouped in the second period from 2006 to 2011. A study carried out by Cid *et al*. (2016) in the Atlantic, concluded that the duration trend was negative, unlike the results obtained in this research, but in the case of extreme storms (Hs > 99.5% Hs), the average duration had increased markedly.

Nevertheless, regarding the significant wave height during storms, there is a predominance of negative trend in the three periods studied. There are high negative trend values as it can be seen in La Palma N in the second period, decreasing the significant wave height by 7 cm per year during storms. This negative trend of significant wave height in mid-latitudes of the Atlantic has been studied in different investigations (Wang *et al*., 2004; Dodet *et al*., 2010). Moreover, as it can be seen in Figure 8, the highest wave heights are found at SIMAR nodes exposed to north waves that present a high energy flow, which could cause this significant increase in wave height (Gonçalves *et al*., 2014). The areas located to the south show a greater increase both in the duration of storms and in significant wave height. This is because, when the model underwent improvements, the height threshold calculated for the entire time series would not be exact, since in the second and third periods the model captures higher wave heights than previously underestimated.

Considering everything studied in this paper, a possible line of research in the future would be to characterize storms in this same area taking into account other oceanographic parameters in addition to those already studied in this work, such as speed and direction of the wind. Furthermore, it would be very interesting to analyse the effects of the North Atlantic Oscillation in the time series. It would also be necessary to establish the values of storm parameters specific to each area and each period to avoid changes in spatial and time resolution affecting the final results. Finally, perform the proper calibration of the model with the instrumental data in advance in order to improve the quality of the starting data (Tomás *et al*., 2004).

6 Conclusion

Numerical models of hindcasting and prediction are the best tool to study long-term trends thanks to the large amount of data available despite the deficiencies described in this research. An adequate calibration of the model with the instrumental data would be necessary to avoid the underestimations seen regarding the buoys. The resolution improvements of the SIMAR series are visible in the case of significant wave height, both in the time series and in the correlations. The SIMAR nodes where these improvements can be seen most, are those located to the south since they are the ones that were making the worst measurements previously.

However, these improvements did not positively affect the peak periods obtained in SIMAR nodes located to the south, like Tenerife S, since the correlations worsened with each improvement.

The significant wave height trend shows negative values in the last two periods with the exception of two SIMAR nodes located at the south of the islands. The average trend in the SIMAR nodes exposed to northern waves presents a clear negative trend of almost 0.6 cm per year, however, in the nodes located to the south of the islands, the negative trend is practically nil, being 0.03 cm per year. Therefore, the significant decrease in wave height will be much more prominent in the areas exposed to northern waves than in the southern areas. In the case of the peak period trends obtained, both in the areas exposed to northern waves and the SIMAR nodes located to the south and less exposed to northern waves, the trend is practically negative, being slightly larger in the south than in the north with values of 0.07 and 0.02 cm a year respectively. In order to obtain the most accurate data possible to take the necessary measures to mitigate the possible future effects of climate change, it would be necessary to properly calibrate the model.

Regarding the trend of storms in the Canary Islands, the duration of storms shows positive trends in practically the 3 periods studied. According to the average value obtained, the duration of storms tends to increase around 0.40 min per year. However, the significant wave height during storms presents negative trends highlighting the last period. According to the average values obtained in the area, the significant wave height during storms tends to decrease about 0.78 cm per year.

Acknowledgment

Thanks to the public entity of Puertos del Estado (Ministerio de Transportes, Movilidad y Agenda Urbana) for the information and data provided of the buoys and SIMAR nodes from HIPOCAST project.

7 References

Allan, J., Komar, P., 2000. Are ocean wave heights increasing in the eastern North Pacific? *Eos, Transactions American Geophysical Union*, 81(47), 561-567.

Anfuso, G., Rangel-Buitrago, N., Cortés-Useche, C., Iglesias Castillo, B., Gracia, F.J., 2016. Characterization of storm events along the Gulf of Cadiz (eastern central Atlantic Ocean). *Int. J. Climatol*. 36, 3690–3707. https://doi.org/10.1002/joc.4585

Bidlot, J. R., Holmes, D. J., Wittmann, P. A., Lalbeharry, R., Chen, H. S., 2002. Intercomparison of the performance of operational ocean wave forecasting systems with buoy data. *Weather and forecasting*, 17(2), 287-310.

Carretero, J.C., Público, E., Weisse, R., Alvarez, E., Público, E., Partenón, A., 2002. A 40 years hindcast of wind, sea level and waves in european waters. *Omae* 2002-28604 1–7.

Ciavola, P., Coco, G. (Eds.), 2017. Coastal storms: processes and impacts. *John Wiley & Sons*.

Cid, A., Menéndez, M., Castanedo, S., Abascal, A.J., Méndez, F.J., Medina, R., 2016. Long-term changes in the frequency, intensity and duration of extreme storm surge events in southern Europe. *Clim. Dyn*. 46, 1503–1516.

Di Paola, G., Rodríguez, G., Rosskopf, C.M., 2020. Short- to mid-term shoreline changes along the south-eastern coast of Gran Canaria Island (Spain). *Rend. Lincei* 31, 89–102.

Dodet, G., Bertin, X., Taborda, R., 2010. Wave climate variability in the North-East Atlantic Ocean over the last six decades. *Ocean Model*. 31, 120–131.

Dorsch, W., Newland, T., Tassone, D., Tymons, S., Walker, D., 2008. A Statistical Approach to Modelling the Temporal Patterns of Ocean Storms. *J. Coast. Res*. 246, 1430–1438.

Godoi, V.A., Bryan, K.R., Gorman, R.M., 2018. Storm wave clustering around New Zealand and its connection to climatic patterns. *Int. J. Climatol*. 38, e401–e417

Gonçalves, M., Martinho, P., Guedes Soares, C., 2014. Assessment of wave energy in the Canary Islands. *Renew. Energy* 68, 774–784.

Grottoli, E., Bertoni, D., Ciavola, P., 2017. Short- and medium-term response to storms on three Mediterranean coarse-grained beaches. *Geomorphology* 295, 738–748. https://doi.org/10.1016/j.geomorph.2017.08.007

Herrera, F. J. G., 2013. Modelización estadística de eventos extremos de oleaje y nivel del mar. Doctoral dissertation, Universidad de Las Palmas de Gran Canaria, 195 pp.

Keim B., Muller R., Stone G., 2004. Spatial and temporal variability of coastal storms in the North Atlantic. *Marine Geology* 210, 7-15.

Komar, P. D., Allan, J. C., 2008. Increasing hurricane-generated wave heights along the US East Coast and their climate controls. *Journal of Coastal Research*, 2008(242), 479-488.

Kossin, J.P., Emanuel, K.A., Vecchi, G.A., 2014. The poleward migration of the location of tropical cyclone maximum intensity. *Nature* 509, 349–352.

Mendoza, E.T., Jimenez, J.A., Mateo, J., 2011. A coastal storms intensity scale for the Catalan sea (NW Mediterranean). *Nat. Hazards Earth Syst. Sci*. 11, 2453–2462.

Nose, T., Webb, A., Waseda, T., Inoue, J., Sato, K., 2018. Predictability of storm wave heights in the ice-free Beaufort Sea. *Ocean Dyn*. 68, 1383–1402. https://doi.org/10.1007/s10236-018-1194-0

Ojeda, E., Appendini, C.M., Mendoza, E.T., 2017. Storm-wave trends in Mexican waters of the Gulf of Mexico and Caribbean Sea. *Nat. Hazards Earth Syst. Sci*. 17, 1305–1317. https://doi.org/10.5194/nhess-17-1305-2017

Pilar, P., Soares, C. G., Carretero, J. C., 2008. 44-year wave hindcast for the North East Atlantic European coast. *Coastal Engineering*, 55(11), 861-871.

Puertos del Estado, 2019. Conjunto de datos SIMAR. *Technical report.*

Ramírez, M., Menéndez, M., Camus, P., Losada, I. J., 2019. Elaboración de la metodología y bases de datos para la proyección de impactos de cambio climático a lo largo de la costa española. *Technical report.*

Rangel-Buitrago, N., Anfuso, G., 2013. Winter wave climate, storms and regional cycles: The SW Spanish Atlantic coast. *Int. J. Climatol*. 33, 2142–2156. https://doi.org/10.1002/joc.3579

Rodríguez, G.R., Cabrera, L., Pacheco, M., 2015. Assessing and modelling annual patterns in wave energy resources off Canary archipelago. *Renew. Energies Offshore - 1st Int. Conf. Renew. Energies Offshore, RENEW* 2014, 105–112.

Tomás, A., Méndez, F.J., Medina, R., Losada, I. J., Menéndez, M., Liste, M., 2004. Bases de datos de oleaje y nivel del mar, calibración y análisis: el cambio climático en la dinámica marina en España. *El Clima entre el Mar y la Montaña*, 155–164.

Wang, X. L., Swail, V. R., 2002. Trends of Atlantic wave extremes as simulated in a 40-yr wave hindcast using kinematically reanalysed wind fields. *Journal of climate*, 15(9), 1020-1035.

Wang, X.L., Zwiers, F.W., Swail, V.R., 2004. North Atlantic Ocean wave climate change scenarios for the twenty-first century. *J. Clim*. 17, 2368–2383.

Yanes, A., Marzol, M. V., Romero, C., 2006. Characterization of sea storms along the coast of Tenerife, the Canary Islands. *J. Coast. Res. Special Issue* 48, 124–128.

Young, I. R., Zieger, S., Babanin, A. V., 2011. Global trends in wind speed and wave height. *Science*, 332(6028), 451-455.

Appendix I

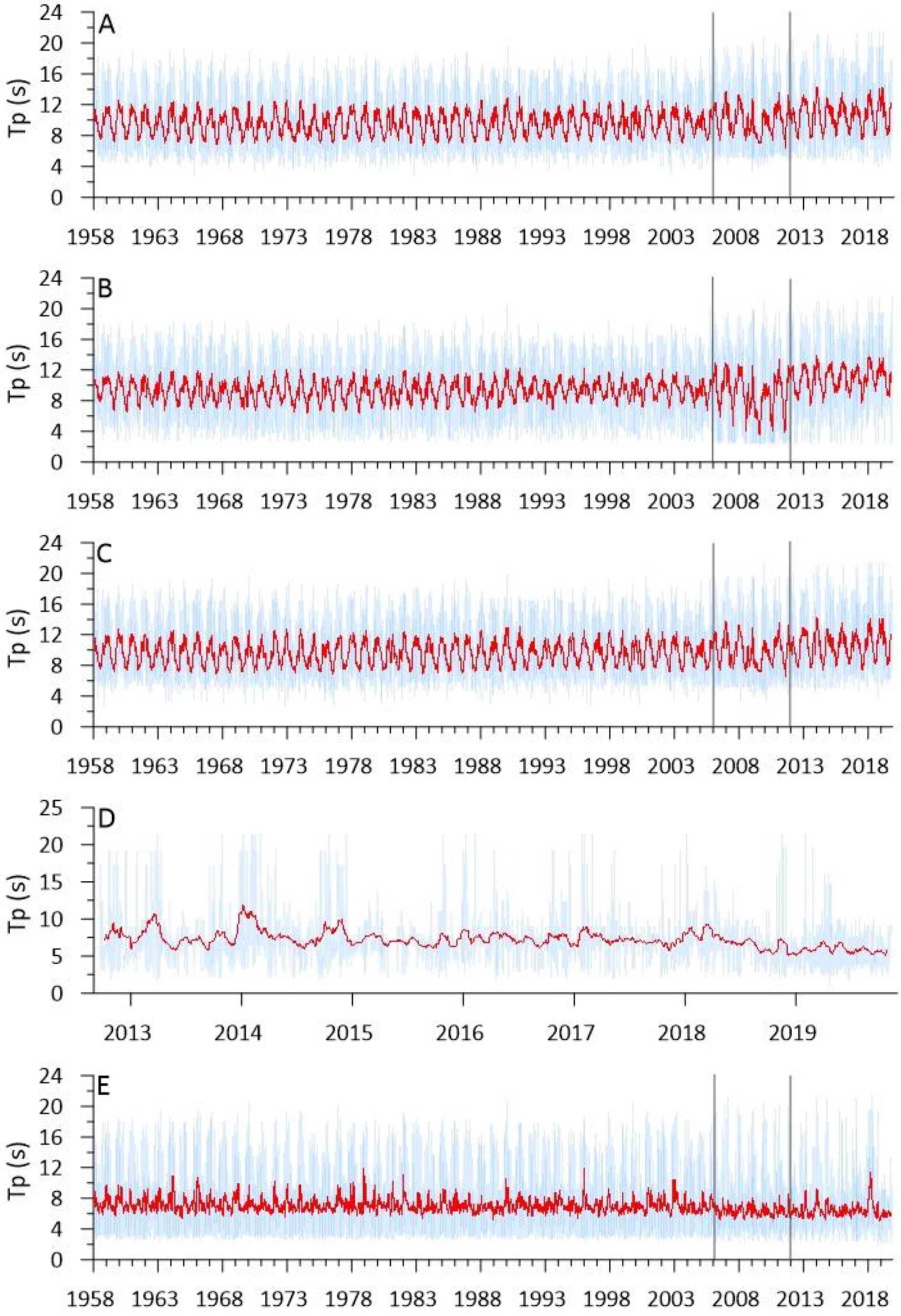
A
B
C
D
E
Tp (s)
0
4
8
12
16
20
24
5
10
15
25
1958
1963
1968
1973
1978
1983
1988
1993
1998
2003
2008
2013
2018
2014
2015
2016
2017
2019

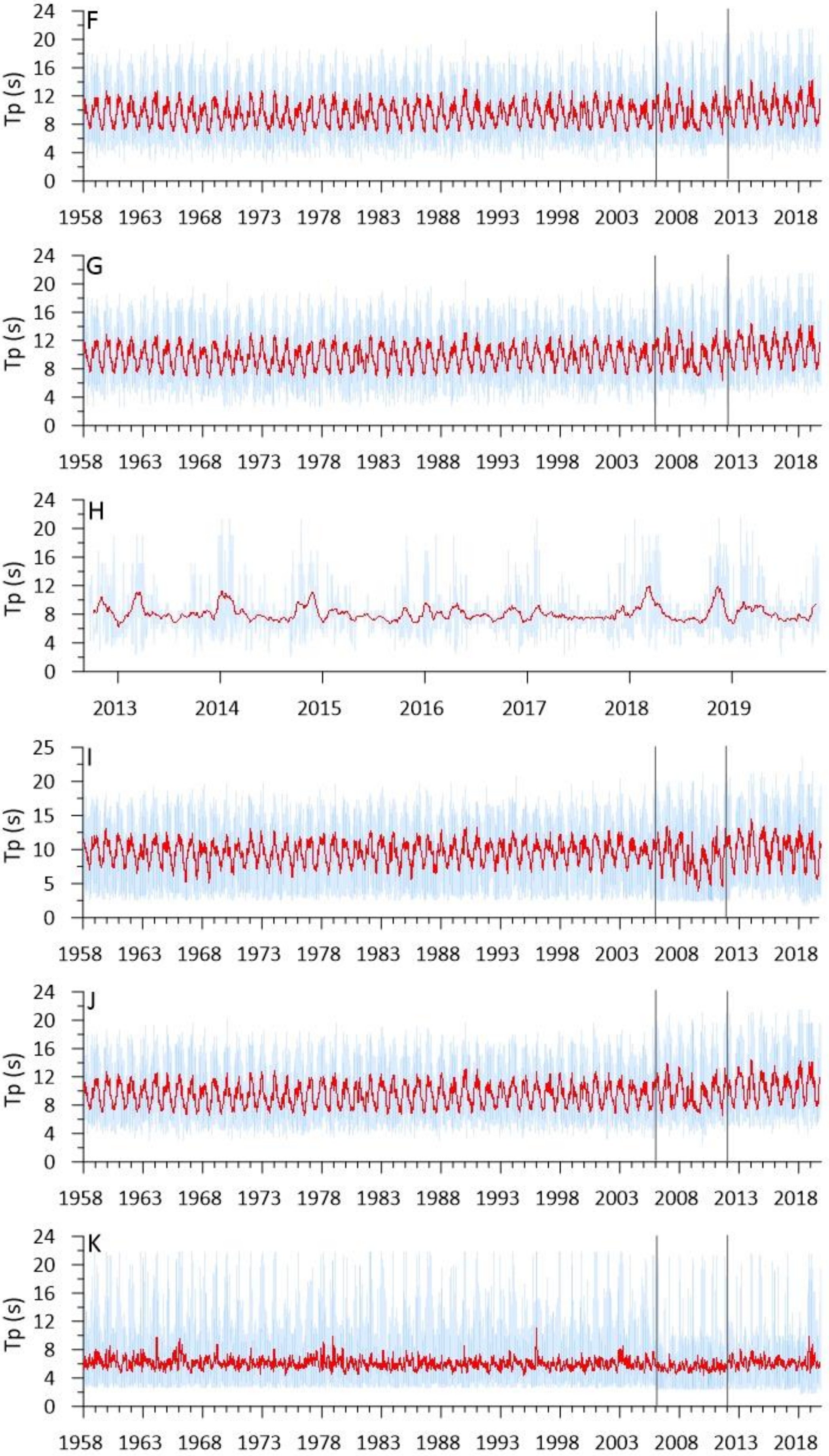
F
G
H
I
J
K
Tp (s)
0
4
8
12
16
20
24
0
5
10
15
20
25
1958
1963
1968
1973
1978
1983
1988
1993
1998
2003
2008
2013
2018
2013
2014
2015
2016
2017
2018
2019